An introduction to random field model to characterize complexity in near - field earthquake slip

Arezou Dorostian[1] and Dr. Mehdi Zaré[2]

Abstract

Although strong ground motion networks are expanding, near-source strong motion recordings are still sparse .In this article it is planned to characterize the level and variability of strong ground motion in near field of large earthquakes due to source effects. We have developed a stochastic rupture model that characterizes the variability and spatial complexity of slip as observed in past earthquakes. We model slip heterogeneity on the fault plane as a spatial random field for 21 near source earthquakes. The data follows a von Karman autocorrelation function (ACF), for which the correlation lengths (*a)* increase with the source dimensions .These stochastic slip distributions are used to develop the temporal behavior of slip using physically consistent with stochastic-dynamic earthquake source models .It means that we can use this model to simulate realistic strong ground motion in order to characterize the variability of source effects in the near-field of large earthquakes. For earthquakes with large fault aspect ratios, we observe substantial differences of the correlation length in the along-strike (*ax*) and downdip (*az)* directions. Increasing correlation length with increasing magnitude can be understood using concepts of dynamic rupture propagation.

The power spectrum of the slip distribution can also be well described with a fractal distribution in which the fractal dimension *D* remains scale invariant, accounting for larger ‘‘asperities ’’ for large-magnitude events.

Our stochastic slip model can be used to generate scenario earthquakes for near-source ground motion simulations.

Keywords*:* Slip heterogeneity, Near source rupture model, Complexity of slip, Random fields, Correlation lengths of asperities, Earthquake rupture dynamics

Introduction

Finite – source images of earthquake rupture show that fault slip is spatially variable at all resolvable scales. Finite – source rupture models are typically derived by inversion of low-pass-filtered strong ground motion recordings [e.g.,Beroza and Spudich,1988], some times augmented with teleseismic data [Hartzell and Heaton,1983;Wald et al.,1991] and/or geodetic measurements [Heaton,1982;Wald and Somerville, 1995; Yoshida et al., 1996]. Some studies derived slip on the fault plane from a forward-modeling approach, other techniques use geodetic data alone to constrain large-scale slip and empirical Green’s function analysis. The rupture complexity inferred from these slip-distribution models has important implication for the dynamic of the earthquake source. Studying the source properties of such well-documented past

[1] PH. D. Student on Geophysics, Seismology; Islamic Azad University, Science and Research Branch

[2] Associate Professor on Engineering Seismology, International Inistitute of Earthquake Engineering and Seismology (IIEES), Tehran, Iran

earthquakes therefore offers the possibility to gain insight into the physics of rupture process. In most cases the differences in the final slip distributions are appreciable, reflecting unmodeled Earth structure, different data processing and weighting the choice of the inversion method, and smoothing or regularization applied during the inversion. The variability in source model provides a means to assess the generally unknown uncertainties of the imaged slip distributions. Rupture variability is of great interest because it strongly influences the level and variability of damaging high-frequency seismic energy radiated by an earthquake [Spudich and Frazer, 1984].

Some theoretical studies of extended-source earthquake models describe heterogeneous slip distributions on fault planes. Andrews [1980b, 1981] showed that a slip spectrum that decays as k^{-2} in the wave number domain leads to far-field displacements that follow the widely observed w^{-2} spectral decay. The fundamental assumption in this model is that individual large and small earthquakes have about the same stress drop. Based on this concept, Herrero and Bernard [1994] introduced the ‘‘k-square’’ model in which the slip spectrum decays as k^{-2} beyond the corner wave number, *kc*, which is related to fault length. In this representation, slip is fractal. The‘‘k-square’’model assumes that the rupture front propagates with constant rupture velocity *vr*, while the rise time depends on wave number. The resulting ground motions follow the w^{-2} decay for far-field displacements, and were used to study directivity effects [Bernard et al., 1996]. Another class of constant stress-drop, extended-source models are the composite source models in which the earthquake is composed of many small events of different size with a fractal size distribution, filling the rupture plane to form the main shock slip distribution [Frankel, 1991; Zeng et al., 1994]. The composite source model has been used success fully to simulate ground motions as well as to invert for earthquake slip distributions [Zeng et al., 1994; Zeng and Anderson, 2000; Su et al., 1996].

All of these models have in common a fractal slip distribution, and hence contain no characteristic length scales to describe the size of asperities (large slip patches, areas of high stress drop). The only length scale in the fractal model is a ‘‘characteristic’’ source dimension, *Lc* (usually fault length) that determines the corner wave number, $k_c \alpha \frac{1}{L_c}$, beyond which the spectra show power law decay.

Somerville et al. [1999] take a deterministic approach to correlate size and number of asperities with seismic moment for a set of finite-source rupture models. They find that the total number of asperities as well as the asperity size increases with seismic moment. The same study also indicates that for a few selected earthquakes the slip distributions may follow a k^{-2} decay in the wave number domain, but there has not yet been an attempt to rigorously verify

the k^{-2} model for published finite-source models. Somerville et al. [1999] propose that the correlation of size of asperity and number of asperities with seismic moment can be used to constrain simulated slip distributions that obey a k^{-2} spectral decay.

In this paper we propose a stochastic characterization of the spatial complexity of earthquake slip as found in finite-source slip inversions (Figure1). We use a spatial random field model in which the slip distribution is described by an autocorrelation function (ACF) in space, or its power spectral density (PSD) in the wave number domain, each parameterized by characteristic length scales ax, az. We compile a data base of 21 near-source rupture models, using for earthquakes, which their hypocenters are <10 Km (Table1), and for each slip model we test whether a Gaussian (GS), an exponential (EX), or a von Karman (VK) ACF provides an appropriate description of the inferred slip distribution. We also examine

the possibility of slip being fractal (meaning that there are no characteristic scale lengths, aside from the source dimensions). Finally , we analyze our measurements of correlation lengths ax, and az, and fractal dimension, D, for dependence on source parameters, i.e., whether scaling laws exist that relate the stochastic source parameters (fractal dimension, corre lation lengths) to deterministic source parameters (fault length, fault width, seismic moment).

Table 1.Source parameters of Finite - Source Rupture Models Used in This Study

No.	*Location*	*Date*	*L*	*W*	*Mw*	*Mo*	*FM*	*REFERENCE*
1	San Fernando	9February1971	19	19	6.8	1.6E+19	RV	Heaton [1982]
2	Tabas	16September1978	95	45	7.1	5.3E+19	RV	Hartzell and Mendoza[1991]
3	ImperialValley	15October1979	42	10	6.5	5.7E+18	SS	Zeng and Anderson[2000]
4	BorahPeak	28October1983	52	26	6.8	1.8E+19	N	Mendoza and Hartzell[1988]
5	Morgan Hill	24 April 1984	30	10	6.2	2.6E+18	SS	Beroza and Spudich[1988]
6	Michoacan	19September1985	180	140	8.0	1.2E+21	RV	Mendoza and Hartzell[1988]
7	Nahinni1	5October1985	40	17	6.7	1.3E+19	RV	Hartzell et al. [1994]
8	Nahinni2	23December1985	48	21	6.8	1.7E+19	RV	Hartzell et al. [1994]
9	N palm Springs	8July1986	22	15	6.1	1.7E+18	OB	Hartzell et al. [1994]
10	Whittier Narrows	10October1987	10	10	5.9	8.7E+17	OB	Hartzell and Iida[1990]
11	Superstition Hills	24 November 1987	24	11	6.6	9.3E+18	SS	Zeng and Anderson[2000]
12	Loma Prieta	18October1989	40	14	6.9	2.4E+19	OB	Beroza[1991]
13	Landers	28June1992	77	15	7.3	7.6E+19	SS	Zeng and Anderson[2000]
14	Northridge	17January1994	18	21	6.7	1.2E+19	RV	Wald[1996]
15	Kobe	17January1995	60	20	6.9	2.8E+19	SS	Zeng and Anderson[2000]
16	Hyuga - Nada1	19October1996	32	32	6.8	1.9E+19	RV	Yagi and Kikuchi[1999]
17	Hyuga - Nada2	2December1996	29	29	6.7	1.3E+19	RV	Yagi and Kikuchi[1999]
18	Izmit (Turkey)	17August1999	125	22	7.4	1.4E+20	SS	Bouchon [2000]
19	Chi-Chi(Taiwan)	20Sep.1999	84	42	7.7	4.6E+20	RV	Zeng and Anderson[2000]
20	Tottori (Japan)	6 October 2000	32	20	6.7	1.4E+19	OB	Ripperger et al. [2007]
21	Parkfield	28 Sep. 2004	40	15	6.1	1.4E+18	SS	Ripperger et al. [2007]

Rv = Reverse, SS = Strike Slip, N = Normal Faulting, OB = Oblique Mechanism

We first discuss the basic concepts of the spatial random field model, and outline the approach we take to determine the best fitting correlation lengths.

It can be applied the technique to published slip distributions, and examine the measured correlation lengths with respect to earthquake source parameters, so we discuss the implications of the result for rupture dynamics.

We can use our model to simulate slip distributions for hypothetical future earthquakes that can be used to calculate synthetic near-field ground motions.

Representing and simulating slip variability with random field models

Spatial random field models are widely used in geosciences to describe quantities with non homogeneous spatial distribution [Goff and Jordan, 1988; Turcotte, 1989; Holliger and Levander, 1992].

They are characterized either in space by an ACF, C (r), or by a PSD, P (k), where is distance and *k* is wave number.

We consider three commonly used correlation functions, the Gaussian, exponential, and von Karman correlation function with the following expressions for

C(r) and P (k): (1)

	C(r)	P(k)
GS	e^{-r2}	$\frac{a_x a_z}{z} e^{-\frac{1}{4}k^2}$
EX	e^{-r}	$\frac{a_x a_z}{(1+K^2)^{\frac{3}{2}}}$
VK	$\frac{G_{H(r)}}{G_{H(\cdot)}}$	$\frac{a_x a_z}{(1+K^2)^{H+1}}$

Where $G_H(r) = r^k K_H(r)$. In these expressions, *H* is the Hurst exponent, K_H is the modified Bessel function of the first kind (order *H*), and k_x and k_z are horizontal and vertical wave numbers, respectively. The characteristic scales are given by the correlation lengths in along-strike and downdip direction, a_x, a_z, respectively and

$$r = \sqrt{\frac{x^2}{a_x^2} + \frac{z^2}{a_z^2}} \quad \textbf{(2)}$$

$$k = \sqrt{a_x^2 k_x^2 + a_z^2 k_z^2}$$

The Hurst exponent H in the expression for the von Karman ACF determines the spectral decay at high wave numbers. For *H*=0.5 the von Karman ACF is identical to the exponential ACF. For a fractal medium, the power spectrum is characterized by a power law decay. In the two-dimensional case, this can be written as [Voss, 1988]

$$P(k) \alpha \frac{1}{k^{B+1}} \alpha \frac{1}{(k_x^2 + k_z^2)^{4-D}} \quad (3)$$

Where

D=E+1-H (4

In (4), *D* is the fractal dimension, *E* the Euclidean dimension of the fractal medium, therefore *D=3-H* for a two dimensional fault plane. From (3) and (4) it follows that $B = 1 + 2H$ .The‘‘k-square’’ model therefore implies *H =1* or equivalently *D=2*.

The differences among the random field models in (1) are illustrated in Figure 2 for four slip distributions with identical phasing. The Gaussian random field seems smooth with little short –scale variation .To estimate the best fitting correlation length for the Gaussian, exponential and von Karman correlation function, we can use a grid-search algorithm by fitting power spectra for discrete values of correlation lengths *a* to measured spectral densities.

We examine average decay properties of the slip using the Fractal Analysis from Circular Average (FACA) method [Anguiano et al., 1994], then we analyze the decay in along-strike and downdip direction separately. In the FACA method, the fractal dimension of a two-dimensional image is estimated from integrated spectral values along a radial, *kr*, and hence only represents average properties of the random field. We extend this approach to more general random fields, parameterized by the ACFs given in (1). This method eliminates possible anisotropy, but it yields more stable average estimates for the decay parameters, which provide a starting point for the subsequent two-dimensional analysis of the slip. We then estimate the best fitting correlation length *ax*, *az*, in along-strike and downdip direction, respectively, by iteratively sweeping through a large range of correlation lengths. This is done for each direction separately using the one-dimensional slice in along–strike or downdip direction.

Application to Finite-Source Models

We estimate parameters of 21 finite-source slip models (Table1) that comprise strike - slip and dip-slip earthquakes from various tectonic regimes. These slip models were derived using a number of inversion techniques, different strategies to stabilize the inversion (regularization and smoothing constraints), and with different spatial sampling .

Slip in earthquakes as imaged by finite-fault inversion techniques is invariably

found to be heterogeneous. The overall dimensions of the rupture planes used in these studies are chosen to be more than large enough to accommodate the entire fault rupture, and therefore may produce slip models with significant portions of low (or even zero) slip towards their edges. Thus, using the dimension of the finite-source model may lead to an overestimate of the "true" rupture area, and hence to scaling laws that do not represent source behavior accurately. This, together with the intrinsically heterogeneous nature of slip in earthquakes, raises the question of how to characterize the spatial extent of the source.

To analyze heterogeneous slip distributions (parameterized by slip values in a two-dimensional array of subfaults) we use *equivalent (effective)* source dimensions, based on definition of autocorrelation width. For a given function, *f*, autocorrelation width, W^{ACF}, is the are under the autocorrelation function of that function,

$$f * f = \int f(u).f(u-x)dx \qquad (5)$$

normalized by the zero-lag value (x=0) of the autocorrelation function (i.e. its maximum):

$$W^{ACF}_{equivalent} = \frac{\int_{-\infty}^{+\infty}(f * f)dx}{f * f\big|x=0} \qquad (6)$$

Using this definition, we calculate the effective length *Leff* (width *Weff*) of the fault from the 1D slip function that is computed by summing the slip values in the individual subfaults in down-dip (along-strike) direction.In order to obtain a uniform representation for all models and to facilitate the comparison among slip models, we bilinearly interpolate all models onto 1x 1 km grid spacing such that the spectral decays are directly comparable.

First we apply the FACA algorithm to estimate the average decay parameters of the slip maps. In simulations the Gaussian ACF is not available model to describe heterogeneous slip in earthquakes, but the exponential and von Karman ACF provide an accurate description of the spectral decay. The inversion often recovers anisotropy with correlation length in along strike direction ,*ax,* being much larger than in down-dip direction, *az*, and the along-strike Hurst exponent *H* is smaller that the downdip Hurst exponent, indicating that a single fractal dimension*(D=3-H)* may not be sufficient to model heterogeneous slipdistributions .

Although the exponential and the von Karman ACF measure very similar correlation lengths, we generally observe that the von Karman ACF returns slightly lower misfits than the exponential ACF due to the additional free parameter (Hurst exponent H) in fitting the decay. It is important that the slip inversion process exerts a strong influence on the measurements of lengths scales (asperity sizes) or fractal dimensions of finite-source rupture models, using the stochastic approach presented in this paper or deterministic approach [Somerville et al., 1999].

The results strongly depend on the limitations of finite-source inversion studies. In these inversions, the rupture plane is discretized into many subfaults where the size of the subfaults may depend on the rupture dimensions, on the availability, spatial distribution and frequency bandwidth of data, and the inversion method used. These data limitations (in spatial distribution, frequency, and quality) leave any slip inversion with a component of the model that can not be constrained by the data. Also, the resolution of the original models of slip may be an isotropic due to gridding or geometric effects. These factors taken together impose strong limitations on the range of spatial parameters present in the inferred slip distributions. Finite -source inversions also include smoothing constrains to stabilize the inversion. The amount of smoothing, however, is often

not a clear–cut objective choice, but rather a subjective one to avoid oscillatory slip maps.

Measurements of asperity size, characteristic scale lengths or decay parameters, based on inferred finite-source models, are therefore only estimates of the true slip complexity during an earthquakes. Nevertheless, we believe that the characteristic scales we find from these slip models are likely to be representative of future earthquakes. In particular, since they are themselves derived from strong motion data, they can be used to simulate complex earthquake slip for strong motion prediction. Now we discuss the estimates of parameters (fractal dimension, *D*, Hurst exponent, *H*, and correlation lengths *a* , *ax* and *az*) for 21 near - source rupture models (Table1). The results are listed in Table2 for each slip model, along with the effective source dimensions, *Leff* and *Weff*. We use these measurements to examine possible dependencies of parameters on source parameters (moment magnitude, *Mw*, fault length, *Lef*, fault width, *Weff*).

Table 2. Estimates of effective source dimensions *Leff* and *Weff*; Fractal Dimension, *D*; Correlation Length, *a*; and Hurst Exponents, *H*, for slip models listed in Table 1

			Fractal	***Exponential***			***Von Karman***					
No.	***Leff***	***Weff***	***D***	***a***	***ax***	***az***	***a***	***ax***	***az***	***H***	***Hx***	***Hz***
1	11.0	11.0	1.8	5.2	5.2	5.0	4.0	4.0	3.8	1.2	1.2	1.2
2	66.0	32.0	2.2	19.5	23.0	12.2	15.8	18.5	10.2	0.8	0.8	0.8
3	22.0	7.0	2.3	4.7	7.2	2.7	3.8	6.7	2.3	0.8	0.7	1.0
4	33.0	21.0	2.1	11.4	13.8	9.2	9.1	10.8	7.4	0.9	0.9	0.9
5	22.0	8.0	2.8	5.5	9.9	3.5	6.5	12.6	3.7	0.3	0.2	0.5
6	136.0	97.0	2.3	50.1	57.4	38.6	41.4	42.2	34.8	0.7	0.9	0.6
7	22.0	11.0	2.6	6.3	7.2	4.8	6.0	7.8	5.1	0.5	0.5	0.5
8	24..0	12.0	2.5	6.7	7.8	4.8	6.7	6.8	5.4	0.5	0.7	0.3
9	15.0	11.0	2.4	5.2	6.4	4.6	4.9	5.6	3.9	0.6	0.8	0.8
10	9.0	8.0	2.2	3.2	3.5	3.0	2.9	3.2	3.4	0.8	0.7	1.2
11	17.0	8.0	2.0	5.4	7.4	3.6	4.2	8.4	2.9	1.0	0.3	1.0
12	26.0	10.0	2.3	6.6	10.0	4.0	5.7	10.0	3.5	0.7	0.5	0.7
13	51.0	11.0	2.3	10.6	24.2	5.1	10.5	17.6	4.5	0.5	0.7	0.7
14	14.0	15.0	2.4	9.4	13.2	5.8	10.8	18.0	6.1	0.3	0.2	0.4
15	37.0	14.0	2.6	9.4	13.2	5.8	10.8	18.0	6.1	0.3	0.2	0.4
16	22.0	24.0	2.2	10.0	9.1	10.6	8.3	7.4	9.1	0.8	0.9	0.8
17	22.0	22.0	2.3	10.1	10.5	10.5	7.7	8.7	9.8	1.0	0.9	0.7
18	85.0	19.0	2.6	17.5	33.2	7.9	17.6	33.9	7.6	0.5	0.5	0.6
19	54.0	27.0	2.4	15.9	22.0	10.3	14.6	19.8	9.5	0.6	0.7	0.6
20	23.0	12.0	2.4	6.6	7.7	4.7	6.6	6.7	5.3	0.5	0.6	0.2
21	25.0	11.0	2.6	6.4	7.1	4.9	6.2	7.5	5.4	0.6	0.5	0.6

Assuming that D>2 is not an artifact of the fault slip inversion method or the inversion for the decay parameters, the observation that D >2 has multiple possible interpretations: (1) non constant stress drop for subevents in a cascade earthquake source model [Frankel, 1991], (2) variability in rise time and/or rupture velocity is mapped into a more heterogeneous slip distribution [Herrero and Bernard, 1994], and (3) surfical geometrical complexity of fault systems extends to depth [Okubo and Aki, 1987; Aviles et al., 1987].

For an earthquake source model consisting of a cascade of ruptures of different sizes the average stress drop over an area on the fault is assumed to be proportional to the standard deviation of the spatial variations in stress drop over that area [Frankel, 1991].

D>2 also implies that stress drop increases as the rupture size becomes smaller (smaller length scales).

Although decreasing stress drop with increasing magnitude is not generally observed, it is in qualitative agreement with a study on strength of asperities [Sammis et al., 1999].

An alternative interpretation for D>2 is that it is an artifact that arises from finite-source inversion methods that do not accurately recover the true variability in rise time or rupture velocity.

Although dynamic rupture modeling indicates that both rise time and rupture velocity are spatially variable over the fault plane, finite-source inversion often treat them as being constant or slowly varying. In order to fit the data, the inversion may therefore map variability in rise time or rupture velocity into a more heterogeneous slip distribution.

Independent evidence for D>2 is found in studies on the geometrical complexity of fault systems [Okubo and Aki, 1987; Aviles et al., 1987]. In particular, Okubo and Aki [1987] find D=1.3 for the mapped fault trace of the San Andreas Fault which translates into D=2.3 for the fault surface using Dsurface = Dtrace + 1 [Okubo and Aki, 1987], consistent with our measurement to D=2.3.

In our opinion, the observation of D>2 is probably attributable to a combination of incorrect mapping of rupture variability into the slip distribution as well as the geometric irregularity of the fault surface that is not accounted for in slip inversions.

We find no evidence that the Hurst exponent depends on magnitude. It is interesting to note that the H estimates are close to H=0.5 for which the von Karman ACF is identical to the exponential ACF, explaining why both the exponential and the von Karman ACF provide similar fits to the observed decay, and generally result in similar correlation length estimates for a given slip model (Table2).

The median estimates for H and D approximately satisfy, D=3-H, although they were derived using different approaches. H ~ 0.8 may again indicate that the constant stress drop model [Andrews, 1980b; Herrero and Bernard, 1994] may not apply to the published slip maps. The observation that H>0.5 becomes important when simulating slip distributions under the condition of finite static self-energy.

Correlation Lengths for Finite-Source Models

In the following discussion, we will focus on the correlation length estimates for the von Karman ACF because (1) the Hurst exponents are found to be close to H=0.5 for which the von Karman ACF is identical to the exponential ACF, leading to similar correlation lengths estimates for the two ACFs and our conclusions hold for either ACF, and (2) we found that the von Karman ACF generally provides a better fit to the observed decay than the exponential ACF or the fractal model, and we therefore adopt the von Karman ACF as our preferred model to describe complexity of earthquake slip. Generally, statistical properties of earthquakes with multiple finite-source slip models seem to be recovered in a consistent manner, and the random field model we propose is able to capture this similarity.

The correlation lengths we obtain are also similar to the asperity dimensions found by Somerville et al. [1999].

While we have estimated stochastic properties of a slip distribution, their measurements are deterministic, and hence the two sets of measurements are no necessarily directly comparable. We find that for slip models with multiple, small asperities, we obtain short correlation lengths and low Hurst exponents. Likewise,

where Somerville et al [1999] find only one or two larger slip patches, we observed longer correlation lengths and larger Hurst exponents. In the deterministic model, the asperity size increases with source dimensions (magnitude), an observation that is confirmed by measurements in that larger earthquakes tend to have longer correlation lengths. We therefore conclude that the "characteristic length scales 'measured in this study agree qualitatively with those by Somerville [1999], though ours is a stochastic representation of slip complexity, whereas theirs is a deterministic one.

Scaling of correlation Lengths with Source Dimensions

Table3.Coefficients for the Scaling of the von Karman Correlation Lengths *a* With Source Parameters; Moment Magnitude, *Mw*, Fault Length, *Leff*, and Fault Width, *Weff*, Separated With Respect to Faulting Style

	Equation	FM	Slope (b1)	Intercept (b0)	Standard Deviation	Correlation Coefficient
Circular Average	log(*a*)=b0+b1*Mw*	SS	0.47	-2.32	0.16	0.87
		DS	0.47	-2.32	0.15	0.89
		AL	0.46	-2.30	0.16	0.86
	a=b0+b1 *Leff*	SS	0.19	1.78	1.30	0.90
		DS	0.28	0.51	1.42	0.93
		AL	0.24	0.74	2.03	0.87
	a=b0+b1 *Weff*	SS	0.94	-2.12	0.12	0.79
		DS	0.43	0.65	0.19	0.95
		AL	0.42	2.24	0.16	0.81
Along-strike	log(*a*)=b0+b1*Mw*	SS	0.60	-2.95	0.21	0.85
		DS	0.47	-2.27	0.15	0.87
		AL	0.52	-2.51	0.20	0.80
	a=b0+b1 *Leff*	SS	0.33	3.61	1.70	0.89
		DS	0.36	0.61	0.75	0.97
		AL	0.35	1.99	1.10	0.92
	a=b0+b1 *Weff*	SS	1.60	-2.57	1.61	0.80
		DS	0.53	1.19	0.88	0.90
		AL	0.48	5.99	1.80	0.78
Downdip	log(*a*)=b0+b1*Mw*	SS	0.30	-1.35	0.16	0.88
		DS	0.34	-1.53	0.18	0.87
		AL	0.34	-1.55	0.19	0.85
	a=b0+b1 *Leff*	SS	0.06	2.76	0.35	0.82
		DS	0.21	1.33	0.79	0.93
		AL	0.15	1.46	1.47	0.87
	a=b0+b1 *Weff*	SS	0.44	-0.06	0.72	0.88
		DS	0.36	0.74	0.80	0.99
		AL	0.36	0.86	0.81	0.98

SS, strikeslip; DS, dipslip; AL, all mechanisms.

A careful analysis of the correlation lengths in Table 2 suggests that *a*, *ax*, and *az* depend on source dimension. The regression of *ax* on fault length *Leff*, and *az* on fault width *Weff* can be used to establish simple scaling relations between these source parameters, which in turn are useful to estimate the correlation length for future earthquakes. The results shown in Table3 suggest a simplified scaling as

$$ax \sim 2.1 + 0.34\ Leff$$
$$az \sim 1.1 + 0.34\ Weff \qquad (7)$$

in which the slope of $b1 = 0.34$ in (7) indicates that correlation lengths scale linearly with effective source dimension.

For earthquakes with small aspect ratio *Leff/Weff*, (7) yields roughly isotropic correlation lengths, while for earthquakes with large aspect ratios (i.e., great strike-slip earthquakes) the correlation length along-strike is larger; (7) also implies the ratio (*ax/Leff) ~ 0.34*. For dip-slip earthquakes, this ratio remains constant over the given magnitude range, while for strike-slip earthquakes the ratio increases with increasing magnitude, with *az/Weff* perhaps saturating at Mw ~ 7.0. In case of circular-averaged *(a)* or along-strike *(ax)* correlation length, the slope of the regression is about 0.5, indicating that the correlation length increases with magnitude in a self-similar fashion. Although the estimates in down dip direction deviate from this apparent self-similarity, We hypothesize a simplified relation between the correlation length and moment magnitude (Table 3) as:

$$\text{Log}(ag) \sim -2.2 + 0.50\,Mw \quad (8)$$

$$\text{Log}(ag) \sim -1.2 + 0.34\,Mw$$

Where *ag* is either circular-averaged or along strike correlation length. The relation in (8) are very similar to results of a study in which the characteristic subevent size*l* was estimated based on source-parameter modeling [Beresnev and Atkinson,2001].They find that *l* sales with magnitude as

$$\text{Log}(l) = -2 + 0.4\,Mw \quad (9)$$

And reanalyzing the catalog of events of Somerville et al [1999] they find

$$\text{Log}(l) = -2 + 0.5\,Mw \quad (10)$$

Interpreting *l* as the asperity size. The simple linear scaling presented in (8), (9), and (10) for the correlation length, subfault size and asperity size, respectively, suggest a fundamental property of extended-source earthquake models, namely, that the characteristic length scales with earthquake magnitude. This property can be used to estimate the characteristics of hypothetical future earthquakes, but it also may be interpreted in terms of the rupture physics.

Additional Data to Constrain Slip Complexity

We propose what additional data may be useful to constrain the fractal dimension or correlation lengths of earthquake slip, and we then discuss the implications of our results for dynamic rupture propagation. Limitations in resolution and accuracy of slip inversions limit the accuracy of the measured fractal dimension and correlation length, particularly at high wave numbers. It is therefore important to identify other data that may be useful to constrain the nature of earthquake slip complexity. Perhaps the most intuitive source of data are measurements of surface slip for large earthquakes. These one-dimensional surface-slip distributions could be analyzed both deterministically (i.e., correlating measured surface slip with imaged slip at depth) and stochastically (i.e., measuring correlation lengths and fractal dimension), and hence could provide additional insight into earthquake source complexity. The disadvantages of such surface-slip measurements, however, are their highly irregular spatial sampling, their large uncertainties [Hough et al., 2000], and the fact that such data exist only for very large earthquakes. We suspect, therefore, such data may be only of limited use to study earthquake source complexity. Analyzing the spatial distribution of microseismicity is another possible approach for studying the spatial complexity of earthquake slip and stress. The spatial distribution of *a* values and *b* values, as imaged by Wiemer and Katsumata [1999], for example, could help to illuminate the spatial complexity of stress drop [Frankel, 1991]. Of course, microearthquake locations are also subject to uncertainties, so it would be most useful to work with a catalog of high-precision earthquake locations, Such data are only available in very well-instrumented regions

(e.g., California, Japan, and Taiwan), but could potentially help to constrain earthquake source complexity, particularly in terms of the geometric fault plane complexities.

Discussion

Uniform correlation lengths for all magnitudes would lead to problems in accommodating the slip (seismic moment) present in large earthquakes. If correlation lengths were about constant over a wide-magnitude range, a large earthquake would be comprised of many small, localized zones in which almost all the moment has to be released. These areas would have very large stress drops, yet would have to rupture in isolation from the surrounding high-slip areas in order to maintain short correlation lengths. It would be difficult to support such behavior from a rupture dynamics view point where neighboring points of the fault interact strongly with each other, and hence are unlikely to allow isolated rupture zones of large stress drops. These arguments lead us to believe that the increasing correlation length for larger earthquakes is not an artifact due to the fault slip inversions (due to coarser fault discretization and longer periods for larger earthquakes), but rather a real property of the earthquake source.

One could argue that the observed correlation length scaling is merely determined by the overall extent of the source (geometry), and that at smaller length scales the slip function is purely self-affine (fractal) with a fractal dimension D arising from scale-independent rupture dynamics. We take an alternative view that the correlation length of the two-dimensional slip distribution of an earthquake is governed by length scales in the rupture process other than the overall source extent and that these may not be purely fractal .An earthquake will contain length scales spanning many orders of magnitudes, from the grain-size scale to total fault length. Geometric irregularities (fault bends, jogs, Offsets) usually occur at lengths scales of 10^{2}–10^{4} m and smaller. These ‘‘static’’ length scales will influence the characteristic lengths during an earthquake. It is also likely that the stress conditions on the rupture plane prior to and during the earthquake significantly influence the final characteristic scales, leading to the observed scaling of the correlation lengths with source dimensions (seismic moment).

Moreover, the dynamics of earthquake rupture will also affect the correlation distances of the final slip distribution. If an earthquake encounters a strong asperity early in the rupture, the seismic load [Andrews, 1985] may not be sufficiently large to break the asperity, and the rupture is arrested early, resulting in a small earthquake with a short correlation distance. If the earthquake manages to break that asperity, its size and moment would grow, and the rupture would have a large area of slip. This scenario would result in a longer correlation distance for a somewhat bigger earthquake. Similarly, late into the rupture (when the seismic load is larger), stress drops may become large locally, and the rupture may become more difficult to stop and hence run to longer distances with significant slip, effectively increasing the correlation length of the final slip for large earthquakes. Therefore, in order to generate heterogeneous slip distributions for scenario earthquakes, with a certain magnitude or length, using Equation (7) and (8) we may calculate the corresponding correlation lengths, then the $P(K)$ is computed and the two dimensional slip function can be obtained .The final slip function in space can then be tapered at edges of the fault to avoid large slip values at the edges of the fault since they lead to infinite large stress changes.

Conclusions

We have developed an approach to characterize spatial complexity of earthquake slip imaged infinite-source rupture inversions. The characterization of slip heterogeneity as a spatial random field

successfully captures correlation lengths. In the case of slip being fractal, we find no indication that the fractal dimension, *D*, depends on other source parameters, and we conclude that *D* is independent of seismic moment. In contrast to the constant stress-drop model *(D=2*), the observation *D>2* may imply size-dependent stress drop for subevents within an earthquake incorrect mapping of variability in rupture velocity and/or rise time into a more heterogeneous slip distribution, or extension of geometric fault trace complexity to depth. Our preferred model is the von Karman ACF for which the correlation lengths *a*, *ax*, and *az* increase with increasing earthquake size. Independent studies [Somerville et al., 1999; Beresenv and Atkinson, 2001] are consistent with the increase of characteristic scale lengths with increasing magnitude that we have found. Simplified scaling relations imply that correlation lengths scale linearly with source dimension, in agreement with Beresenv and Atkinson, [2001].The spatial random field model for earthquake slip may be used to generate scenario earthquakes for strong motion prediction. We generate spatially variable slip distributions using the spectral synthesis method. It is important to note, however, that each realization of heterogeneous earthquake slip is subject to the condition that the static strain energy associated with the slip distribution remains finite. This condition ensures that stresses can not become infinite (though locally they may become very large). Strong motion synthetics computed from these simulated slip distributions, assuming simple kinematic rupture parameters show the utility of the model for strong motion prediction.

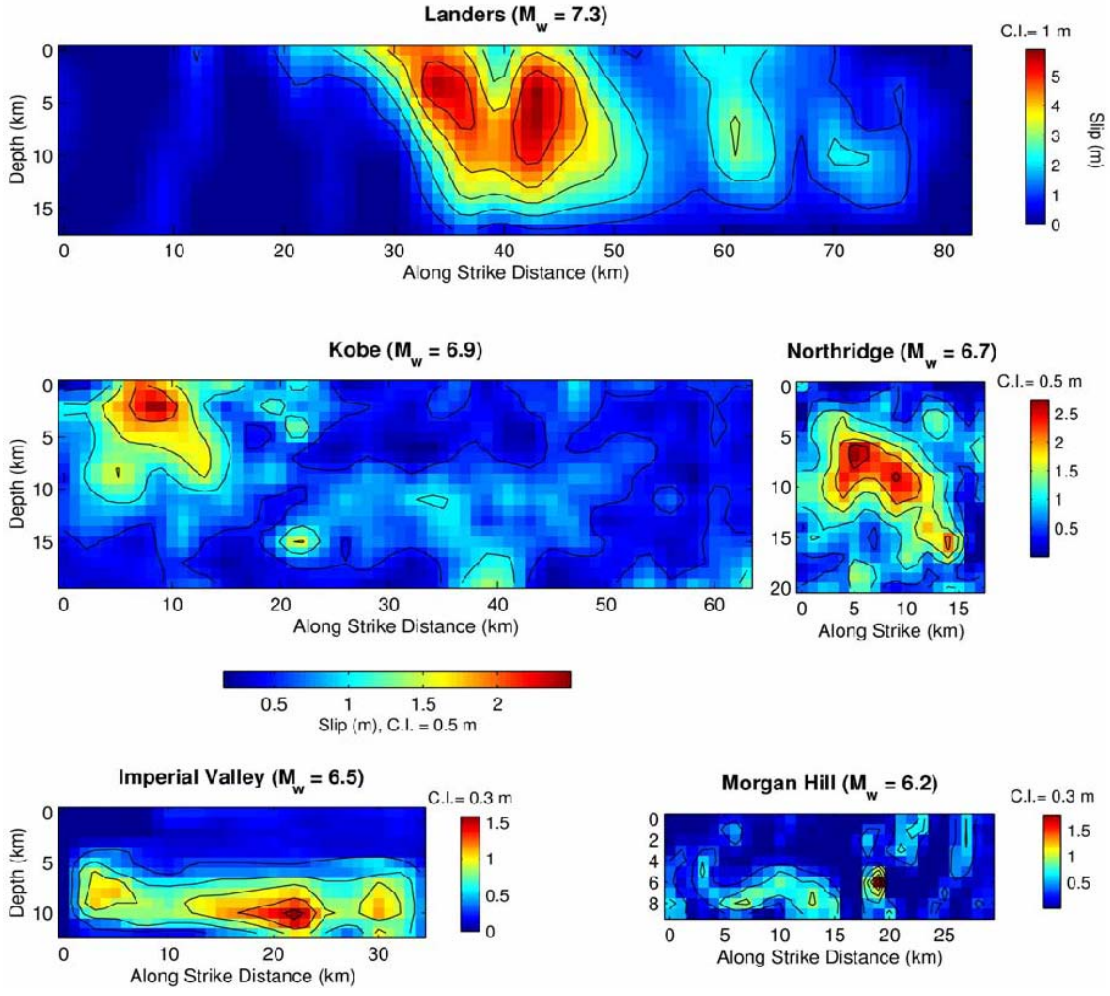

Figure1.Slip distributions from finite-source models, illustrate the variability of slip on the rupture plane.

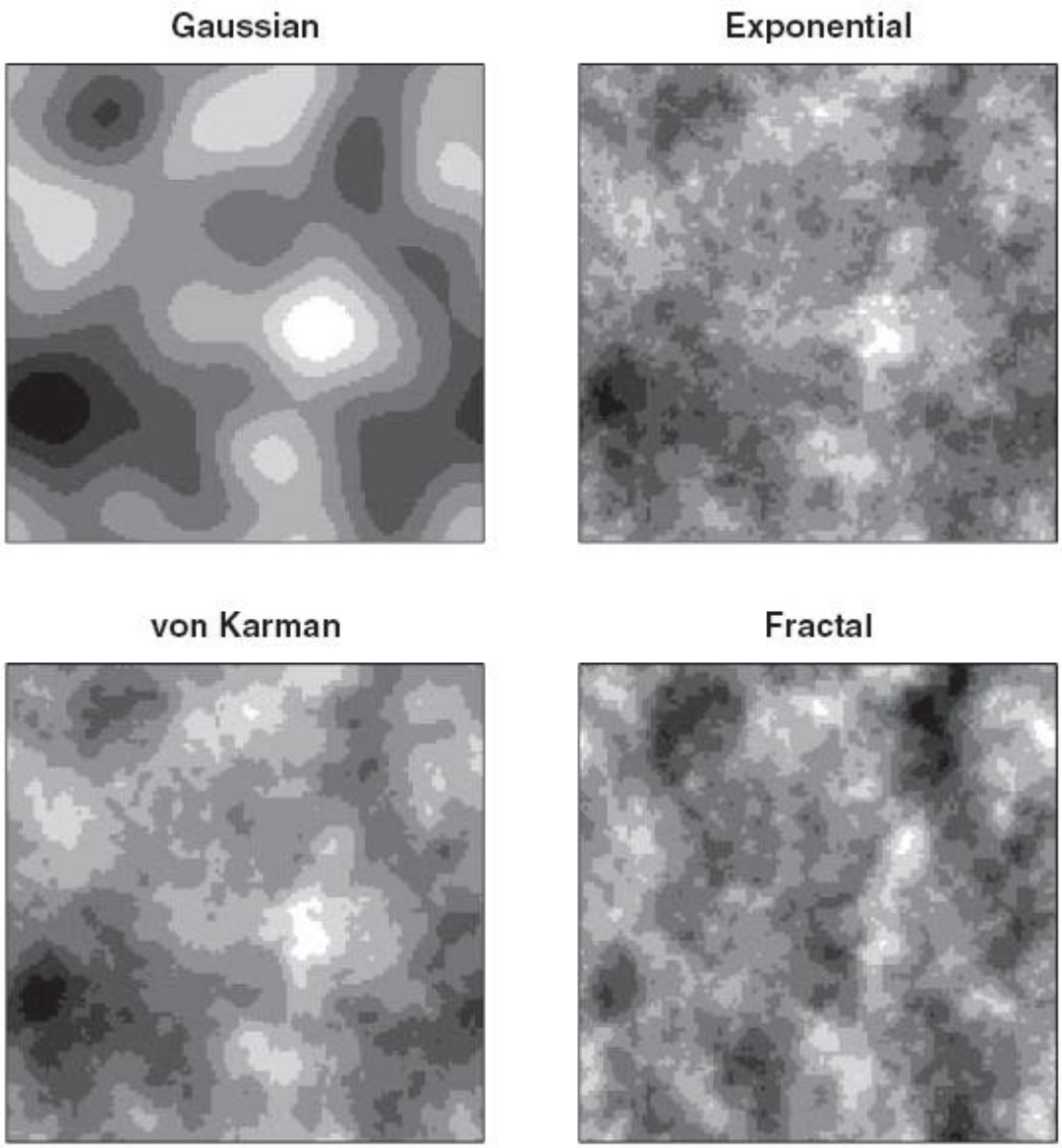

Figure2. An example of the spatial random field model, generated with identical phasing to facilitate the comparison. The correlation lengths are considered *a* = 5 km for the Gaussian, exponential, and von Karman ACF; for the von Karman model, *H*=0.8; and for the fractal case, *D* = 2.2.

References

-Andrews, D.J., 1980b, A. stochastic fault model, I, Static case, J. Geophys. Res., 85, 3867 – 3877,

-Andrews, D. J., 1981, A stochastic fault model, II Time – dependent case, J. Geophys. Res., 86, 10,821–10,834.

-Anguiano, E., Pancorbo,M., and Aguilar, M., 1994, Pitfalls in the fractal characterization of real microscopic surfaces by frequency analysis and proposal of a new method, in Fractals in the Natural and Applied Science, edited by M. M. Novak, pp. 37-46, Elsevier Sci., New York.

-Aviles, C. A., Scholz, C.H., and Boatwright, J., 1987, Fractal analysis applied to characteristic segments of the San Andreas Fault, J. Geophys .Res., 82 ,331-344.

-Beresenv, I., and Atkinson, G., 2001, Subevent structure of large earthquakes: A ground motion perspective, Geophys. Res. Lett, 28, 53-56.

-Bernard, P., Herrero, A., and Berge, C., 1996, Modeling directivity of heterogeneous earthquake rupture, Bull. Seismol. Soc. Am., 86, 1149–1160.

-Beroza, G. C., 1991, Near source modeling of the Loma Prieta earthquake: Evidence for heterogeneous slip and implications for earthquake hazard, Bull. Seismol. Soc. Am.,

81, 1603-1621.

-Beroza, G. C., and Spudich, P., 1988, Linearized inversion for fault rupture behavior: Application to the 1984 Morgan Hill, California, earthquake, J.Geophys. Res., 93, 6275–6296.

-Bouchon, M., Toksoz, M. N., 2000, Seismic imaging of 1999 Izmit Turkey) rupture inferred from near-fault recordings, Geophys. Res. Lett., 27, 3013-3016.

-Frankel, A., 1991, High-frequency spectral fall-off of earthquakes fractal dimension of complex rupture, b value, and the scaling of strength on faults, J. Geophys. Res., 96, 6291–6302.

-Goff, J. A., and Jordan, T. H., 1988, Stochastic modeling of seafloor morphology: Inversion of sea beam data for second - order statistics, J. Geophys. Res., 93, 13, 589–608.

-Hartzell, S. H., and Heaton, T. H., 1983, Inversion of strong ground motion and teleseismic wave- form data for the fault rupture history of the 1979 Imperial Valley, California, earthquake, Bull. Seismol. Soc. Am., 73, 1553– 1583.

-Hartzell, S. H., and Iida, M., 1990, Source complexity of the 1987 Whittier Narrows California, earthquake from the inversion of strong motion records, J. Geophys Res., 95, 12, 475-12,485.

-Hartzell, S. H., Langer, C., and Mendoza, C., 1994, Rupture histories of eastern North American earthquakes, Bull. Seismol. Soc. Am., 84, 1703-1724.

-Heaton, T. H., 1982, The 1971, San Fernando earthquake: A double event? , Bull. Seismol. Soc. Am., 72, 2037–2062.

-Herrero, A., and Bernard, P., 1994, A kinematic self – similar rupture process for earthquakes, Bull. Seismol. Soc. Am., 84, 1216–1228.

-Holliger, K., and Levander, A. R., 1992, A stochastic view of lower crustal fabric based on evidence from the Ivrea zone, Geophys. Res. Lett., 11, 1153–1156.

-Hough, S. E., and Scientists from the U. S. Geological Survey, 2000, Southern California Earthquake Center, and California Division of Mines and Geology Preliminary repot on the 16 October 1999, M=7.1 Hector Mine, California, earthquake, Seismol. Res. Lett., 71, 111-23.

-Mendoza, C. and Hartzell, S. H., 1988, Inversion for slip distribution using teleseismic P wave-forms: North Palm Springs, Borah Peak, and Michoacan Earthquakes, Bull. Seismol. Soc. Am., 78, 1092-1111.

-Okubo, P. G., and Ak i, K., 1987, Fractal geometry in the San Andreas Fault system, J. Geophys system, Res., 92, 345–355.

-Ripperger, J., Mai, P. M., Ampuero, J. P., and Giardini, D., 2007, Earthquake source Characteristics from dynamic rupture with constrained stochastic fault stress, J.Geophys. Res., 112, B04311, doi: 10. 1029/2006 JB 004515.

-Sammis, C. G., Nadeau, R. M. and Johnson, L. R., 1999, How strong is an asperity? J. Geophys. Res., 104, 10, 609–619.

-Sekiguchi, H. and Iwata, T., 2002, Rupture process of the 1999 Kocaeli, Turkey, earthquake estimated from strong-motion waveforms, Bull. Seismol. Soc. Am., 92, 300-311.

-Somerville, P. G., Irikura, K., Graves, R., Sawada, S., Wald, D. J., Abrahmson, N., Iwasaki, Y., Kagawa, T., Smith, N. and Kowada, A., 1999, Characterizing crustal earthquake slip models for the prediction of strong ground motion, Seismol Res. Lett., 70, 59–80.

-Spudich, P., and Frazer, N., 1984, Use of ray theory to calculate high-frequency radiation from earthquake sources having spatially variable rupture velocity and stress drop, Bull Seismol. Soc. Am., 74, 2061–2082

-Su, Y., Anderson, J. G., and Zeng, Y., 1996, Comparison of strong and weak motion site amplifications from Northridge earthquake sequence, Eos Trans. AGU, 77, 494.

-Turcotte, D. L., 1989, Fractals in geology and geophysics, Pure Appl. Geophys., 131,171–196.

-Voss, R. F., 1991, Fractals in nature: From characterization to simulation, in The Science of Fractal Images, edited by H.-O. Peitgen and D.Saupe, pp. 21–70, Springer-Verlag, New York.

-Wald, D. J. and Somerville, P. G., 1995, Variable-slip rupture mode of the great 192 Kanto, Japan earthquake: Geodetic and body-wave form analysis, Bull. Seismol. Soc. Am., 85, 159–177.

-Wald, D. J., Helmberger, D. V., and Heaton, T. H. 1991, Rupture model of the 1989 Loma Prieta earthquake from the inversion of strong-motion and broad band teleseismic data, Bull. Seismol.Soc.Am., 81, 1540 – 1572.

-Wald, D. J., Heaton, T. H. and Hudnut, K. W., 1996, The slip history of the 1994 Nothridge,

California, earthquake determined from strong-motion, teleseismic, GPS, and leveling data, Bull. Seismol.Soc.Am, 86, 49-70.

-Wiemer, S., and Katsumata, K., 1999, Spatial variability of seismic parameters in after shock zones, J. Geophys. Res., 104, 13, 135152.

-Yagi, Y. and Kikuchi, M., 1999, Comparison of the coseismic rupture with the after shock distribution in the Hyuga-nada earthquake of 1996, Geophys. Res.Lett, 3161-3164.

-Yoshida, S., Koketsu, K., Kato, T., Shibazaki, B., Sagiya, T. and Yoshida, Y., 1996, Joint inversion of near–and far - field waveforms and geodetic data for the rupture process of the 1995 Kobe earthquake, J. Phys. Earth, 44, 437– 454 .

-Zeng, Y., and Anderson, J. G., 2000, Earthquake source and near-field directivity modeling of several large earthquakes, in EERI 6th International Conference on Seismic Zonation, Palm Springs.

-Zeng, Y., Anderson, J. G., and Guang, Y., 1994, A composite source model for computing realistic synthetic strong ground motions, Geophys. Res, Lett, 21, 725–728.